Organotin-Drug Interactions. Organotin Adducts of Tenoxicam: Synthesis and Characterization of the First Organotin Complex of Tenoxicam

by **Mavroudis A. Demertzis**[a])*, **Sotiris K. Hadjikakou**[a]), **Dimitra Kovala-Demertzi**[a])*, **Aglaia Koutsodimou**[b]), and **Maciej Kubicki**[c])

[a]) Inorganic and Analytical Chemistry, Department of Chemistry, University of Ioannina, 45100 Ioannina, Greece

[b]) NRPCS Democritos, Institute of Physical Chemistry, 15310 Aghia paraskevi Attikis, Greece

[c]) Department of Chemistry, A. Mickiewicz, University, ul. Grunwaldzka 6, 60-78-Poznan, Poland

The synthesis and spectral characterization of the novel organotin complexes $[SnBu_2(ten)]$ (**1**) and $[SnBu_2(Hten)_2]$ (**2**) of the potent and widely used anti-inflammatory drug tenoxicam (H_2ten) are reported. A crystal-structure determination of **1** showed that, in this complex, the ligand is doubly deprotonated at the hydroxy O-atom and the amide N-atom and is coordinated to the $SnBu_2$ fragment *via* four- and six-membered chelate rings. An extended network of Sn–O–Sn, C–H···O and C–H···π contacts lead to aggregation and a supramolecular assembly. Potentiometric titrations in nonaqueous solutions support the ionization of the drug by removal of the second H-atom, the amide H-atom, in the presence of the diorganotin(IV) fragment. The K_a values of the poorly H_2O-soluble drug tenoxicam were obtained spectrophotometrically in aqueous solutions of constant ionic strength.

1. Introduction. – Tenoxicam (=4-hydroxy-2-methyl-*N*-(pyridin-2-yl)-2*H*-thieno[2,3-*e*]-1,2-thiazine-3-carboxamide 1,1-dioxide; H_2ten) is a new non-steroidal drug that has anti-inflammatory, analgetic, and antipyretic effects. The drug is widely used in the treatment of rheumatic diseases [1]. It is a derivative of oxicam with a thiophene ring replacing the benzene ring in piroxicam. Both piroxicam and tenoxicam are the most famous members of this group. Tenoxicam acts by inhibiting enzymes involved in the biosynthesis of prostaglandins such as cyclooxygenase, which catalyzes the formation of cyclic endoperoxides [2][3].

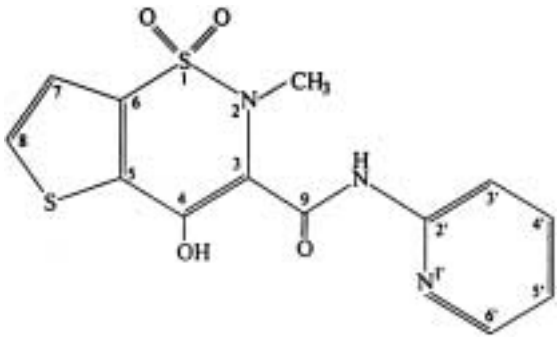

The drug, with four donor atoms and several possible isomers [4], is suggested to react as a singly deprotonated bidentate chelate ligand, through the enolate O-atom

and the amide O-atom, towards copper(II), iron(III), cobalt(II), nickel(II), and manganese(II) [5].

The weakly basic pyridinyl group gives rise to a zwitterion [6], resulting in an extended electron conjugation through the molecule and making the acidity of the enolic group remarkably higher [7]. The acid-base behavior of tenoxicam was also studied, and apparent pK_a values were reported [4][7].

Organotin(IV) compounds form an important series of compounds and have been receiving increasing attention in recent years, not only because of their intrinsic properties, but also owing to the importance of tin-based antitumor drugs. Some examples find wide applications as catalysts and stabilizers, and certain derivatives are used as biocides, as antifouling agents, and for wood preservation. In recent years, investigations have been carried out to test their antitumor activity, and it has been observed that indeed several diorganotin adducts, as well as triorganotin species, show potential as antineoplastic (mainly antileukemic) agents [8][9].

We have developed an interest in the coordination chemistry and anti-inflammatory properties of non-steroidal anti-inflammatory drugs with transition- [10] and non-transition-metal [11] ions, and report here the interaction of $SnBu_2Cl_2$ with tenoxicam (H_2ten) and the crystal structure of the complex $[SnBu_2(ten)]_n$. It is the first structure of a tenoxicam complex with organotin and the first case where tenoxicam acts as a doubly deprotonated tridentate ligand. Potentiometric titrations in nonaqueous solutions support the ionization of a second H-atom from the drug, *i.e.* the amide-group H-atom, in the presence of the diorganotin(IV). Further, real concentration or mixed protonation constants for tenoxicam were determined spectrophotometrically in pure aqueous solutions of constant ionic strength.

Experimental Part

General. All the chemicals used were of high purity and purchased from *Fluka*, *Merck*, and *Aldrich*. Solvents were purified and dried according to standard procedures. Tenoxicam was a gift from *HELP EPE*, Ioannina, Greece, and was recrystallized twice from EtOH. pH Values: *Metrohm 691* pH meter. *Jasco UV/Vis/NIR-V-570* spectrophotometer. IR and far-IR spectra: *Perkin-Elmer Spectrum-JX-FT-IR* spectrophotometer; in KBr or polyethylene discs. Elemental analyses: *Carlo Erba EA* (model *1108*).

*Dibutyl[4-(hydroxy-*κO*)-2-methyl*-N-*(pyridin-2-yl-*κN*)-2*H-*thieno[2,3-*e*]-1,2-thiazine-3-carboxamide 1,1-Dioxidato(2−)-*κN^3*]tin* ([$SnBu_2$(ten)]; **1**). To a soln. of tenoxicam (H_2ten; 0.168 g, 0.5 mmol) in benzene (20 ml) $SnBu_2O$ (0.124 g, 0.5 mmol) was added, and the mixture was refluxed for 4 h under a *Dean-Stark* trap. The clear soln. was evaporated, the resulting powder dissolved in MeOH (15 ml), filtered off, and slowly evaporated to 2–3 ml. The final pale yellow product was filtered off and dried *in vacuo* over silica gel: **1**. M.p. 168–170°. Anal. calc. for $C_{21}H_{27}N_3O_4S_2Sn$: C 44.39, H 4.78, N 7.39, S 11.28; found: C 44.63, H 4.89, N 7.10, S 11.47.

Crystals of **1** suitable for X-ray analysis were obtained by slow evaporation of a fresh MeOH/MeCN soln.

*Dibutylbis[4-(hydroxy-*κO*)-2-methyl*-N-*(pyridin-2-yl-*κN*)-2*H-*thieno[2,3-*e*]-1,2-thiazine-3-carboxamide 1,1-Dioxidato]tin* ([$SnBu_2$(Hten)$_2$]; **2**). Exactly as described for **1**, with H_2ten (0.168 g, 0.5 mmol), benzene (20 ml), and $SnBu_2O$ (0.062 g, 0.25 mmol): **2**. Pale green-yellow solid. M.p. 161–163°. Anal. calc. for $C_{34}H_{38}N_6O_8S_4Sn$: C 45.10, H 4.23, N 9.28, S 14.16; found: C 45.03, H 4.16, N 8.77, S 14.58.

Slow crystallization of MeOH/MeCN solns. of **2** yielded pale yellow crystals of **1** and powder of tenoxicam.

Crystal-Structure Determination of **1** (see *Table 1*). X-Ray diffraction data were collected on a *KUMA KM4* κ-geometry diffractometer [12a], with graphite-monochromated MoK_α (λ 0.71073 Å) radiation. The unit-cell dimensions were calculated by least-squares fitting to 39 automatically centered reflections ($12.4° \leq 2\theta \leq 37.8°$). Relevant crystallographic data, together with data-collection and structure-refinement details are listed in

Table 1. The 2θ-θ scan method and a variable scan speed ranging from 1.2 to 24°/min, depending on reflection intensity, were applied. Three control reflections (222, 006, and 026) were measured after every 100 current measurements. Intensity data were collected for *Lorentz* and polarization effects [12a]. The structure was solved by the *Patterson* method with the SHELXS86 program [12b]. The full-matrix least-squares method was used for refinement with SHELXL93 [12c]. Scattering factors incorporated in SHELXL93 were used. The function $\Sigma_w (|F_o|^2 - |F_c|^2)^2$ was minimized with $w^{-1} = [\sigma^2(F_o)^2 + 0.050P^2]$, where $P = \max(F_o^2,0) + 2Fc^2/3)$. The positions of the H-atoms were calculated from geometry and treated as 'riding model'. The U_{iso} values for H-atoms were assumed as 1.2 times U_{eq} of their carriers. Two reflections were excluded from the reflection file, due to their large ($|F_o^2| - |F_c^2|$) differences. The relatively high residual electron density, away from the complex, was interpreted as a disordered solvent (MeOH) molecule. Crystallographic data (excluding structure factors) for **1** have been deposited with the Cambridge Crystallographic Data Centre as deposition No. CCDC-150096. Copies of the data can be obtained, free of charge, on application to the CCDC, 12 Union Road, Cambridge CB2 1EZ, UK (fax: +44(1223)336033; e-mail: deposit@ccdc.cam.ac.uk).

Table 1. *Crystal Data and Structure Refinement for [SnBu$_2$(ten)]* (**1**)

Empirical formula	$Sn(C_4H_9)_2(C_{13}H_9N_3O_4S_2) \cdot 1/2\ (CH_3OH)$
Formula weight	575.27
Crystal system	tetragonal
Space group	*I*-4
a/Å	19.497(3)
c/Å	13.131(2)
V/Å^3	4991.5
Z	8
D_{calc}/g·cm^{-3}	1.53
F(000)	2332
Γ/mm^{-1}	1.22
Crystal size/mm	0.4 × 0.3 × 0.25
Temperature/K	293(2)
Wavelength/Å	0.71073
2θ Range/°	1.5 – 30
hkl Range	$0 < h < 27$
	$0 < k < 27$
	$0 < l < 18$
Decay of standards	1%
Reflections: collected	4010
Number of parameters	290
R(*F*)	0.028
$wR(F^2)$ ($F_o \geq 4\sigma(F_o)$)	0.077
Goodness of fit	1.12
max/min resd. dens./e Å^{-3}	0.99/ – 1.00

Protonation Constants and Potentiometric Titration. The low solubility of tenoxicam and its low log $K_{\alpha 2}$ value is the reason for using spectrophotometry to find the protonation constants of the molecule. Aq. tenoxicam solns. of constant ionic strength were used to determine protonation constants by a methodology explained elsewhere [13a]. All solns. were prepared with distilled H_2O obtained from a borosilicate auto-still (*Jencons Ltd.*). The stock soln. ($1 \cdot 10^{-3}$ M) of tenoxicam (H_2ten) was initially prepared by suspending for 1 h the appropriate amount of the drug in $2 \cdot 10^{-3}$ M KOH. In the absence of atmospheric CO_2, the soln. remained clear and stable for long periods. Exactly $5 \cdot 10^{-5}$ M working tenoxicam solns. having different H^+ ion concentrations and constant ionic strengths ($\mu = 0.1$ or 1.0) were then prepared with standard HCl or KOH and KCl solns. All measurements were made at 25°, and the absorption spectra were collected in the range 240 – 450 nm.

A rearrangement [13b] of the well-known relationship (*Eqn. 1* or *2*) (where ε_o, $\varepsilon_{(Hten^-)}$, $\varepsilon_{(H_2ten)}$ and $\varepsilon_{(H_3ten^+)}$ are the absorption coefficients of the observed soln., the negatively ionized, molecular, and positively charged species, resp.), in the form of *Eqn. 3* or *4* was used to determine $K_{\alpha 1}$ and $\varepsilon_{(H_2ten)}$ values from *Eqn. 3* as well as $K_{\alpha 2}$ and $\varepsilon_{(H_3ten^+)}$ values from *Eqn. 4*. The $\varepsilon_{(Hten^-)}$ value can be securely obtained from the absorption spectra of

tenoxicam that completely coincide with each other at pH > 8. According to *Eqns. 1* and *2*, only relatively low errors may accompany the $\varepsilon_{(H_2ten)}$ and K_{a1}, but estimation of the $\varepsilon_{(H_3ten^+)}$ and K_{a2} values is impossible because extremely acidic solns. have to be used.

$$Ka1 = [H_3O^+]\frac{\varepsilon_{(H_2ten)} - \varepsilon_o}{\varepsilon_o - \varepsilon_{(Hten^-)}} \quad (1) \quad \text{or} \quad Ka2 = [H_3O^+]\frac{\varepsilon_{(H_3ten^+)} - \varepsilon_o}{\varepsilon_o - \varepsilon_{(H_2ten^-)}} \quad (2)$$

$$\varepsilon_o = \varepsilon_{(H_2ten)} - Ka1\frac{\varepsilon_o - \varepsilon_{(Hten^-)}}{[H_3O^+]} \quad (3) \quad \text{or} \quad \varepsilon_o = \varepsilon_{(H_3ten^+)} - Ka2\frac{\varepsilon_o - \varepsilon_{(H_2ten)}}{[H_3O^+]} \quad (4)$$

Potentiometric titrations in non-aq. solns. support the ionization of a second H-atom from the drug. Almost universally, the glass electrode is the most important tool for pH measurements in aq. solns. However, both tenoxicam and $SnBu_2Cl_2$ are poorly soluble in H_2O. Therefore, $CHCl_3$/MeOH 1:1 (*v*/*v*) was used as an appropriate solvent. The pH values obtained in non-aq. solvents are referred to as 'apparent pH' values when the glass electrode was standardized with an aq. soln. [13c].

Results and Discussion. – *Protonation Constants.* In aqueous solns, only three independent species of tenoxicam ($Hten^-$, H_2ten, and H_3ten^+) become visible as shown by the absorption spectra in *Fig. 1*. Therefore, there are two distinct steps of protonation, and the equilibria between the species are given by *Eqns. 5* and *6*.

$$Hten^- + H_3O^+ \overset{K_{a1}}{\rightleftharpoons} H_2ten + H_2O \quad (5)$$

$$H_2ten + H_3O^+ \overset{K_{a2}}{\rightleftharpoons} H_3ten^+ + H_2O \quad (6)$$

The concentration protonation constants of tenoxicam $K_{\alpha1}$ and $K_{\alpha2}$, for $\mu = 0.1$, were determined, and the 95% confidence limits of their logarithms were found to be equal to 5.22 ± 0.06 and 0.72 ± 0.02 ($n = 8$) with relative standard deviations (r.s.d.) of 1.77 and 4.10%, respectively. Further, for ionic strength $\mu = 1.0$, a concentration protonation constant $K_{\alpha1}$ with $\log K_{\alpha1} = 5.31 \pm 0.01$ and an r.s.d. of 0.04% ($n = 5$ at 95% level) was determined, while a mixed protonation constant $K_{\alpha2}$ with $\log K_{\alpha2} = 1.14 \pm 0.02$ and r.s.d. = 2.64% ($n = 10$ at 95% level) was found.

Titration in Organic Solvents. Potentiometric titrations in $CHCl_3$/MeOH 1:1 (*v*/*v*) were performed to support the ionization from the drug of the second H-atom, the amide-group H-atom, in the presence of the diorganotin(IV) fragment (see *Fig. 2*). During an acid-base titration, the apparent pH values are very useful, since they can give information about the kind and the relative extent of a reaction. Thus, the pH values of tenoxicam titrated with KOH lie much lower than those of the solvent alone (see *Fig. 2*, *a* and *b*). This feature and the rapid pH change in the immediate vicinity of the equivalence point show that the neutralization process is effectively completed and involves only one proton of tenoxicam.

For an amount of $SnBu_2Cl_2$ equivalent to that of tenoxicam, the titration curve presents two neutralization steps corresponding to the hydrolysis steps of the molecule for its two Cl-atoms (*Fig. 2*, *c*). The inflection point of the second step is weak and appears when exactly 2 equiv. of base have been spent. The first inflection point corresponds to an amount of titrant larger than the stoichiometric one because of a simultaneous contribution of protons from the second step of hydrolysis.

The titration curve for a mixture of equivalent amounts of tenoxicam and $SnBu_2Cl_2$ also shows two steps (*Fig. 2*, *d*). The first inflection point of this curve coincides with the

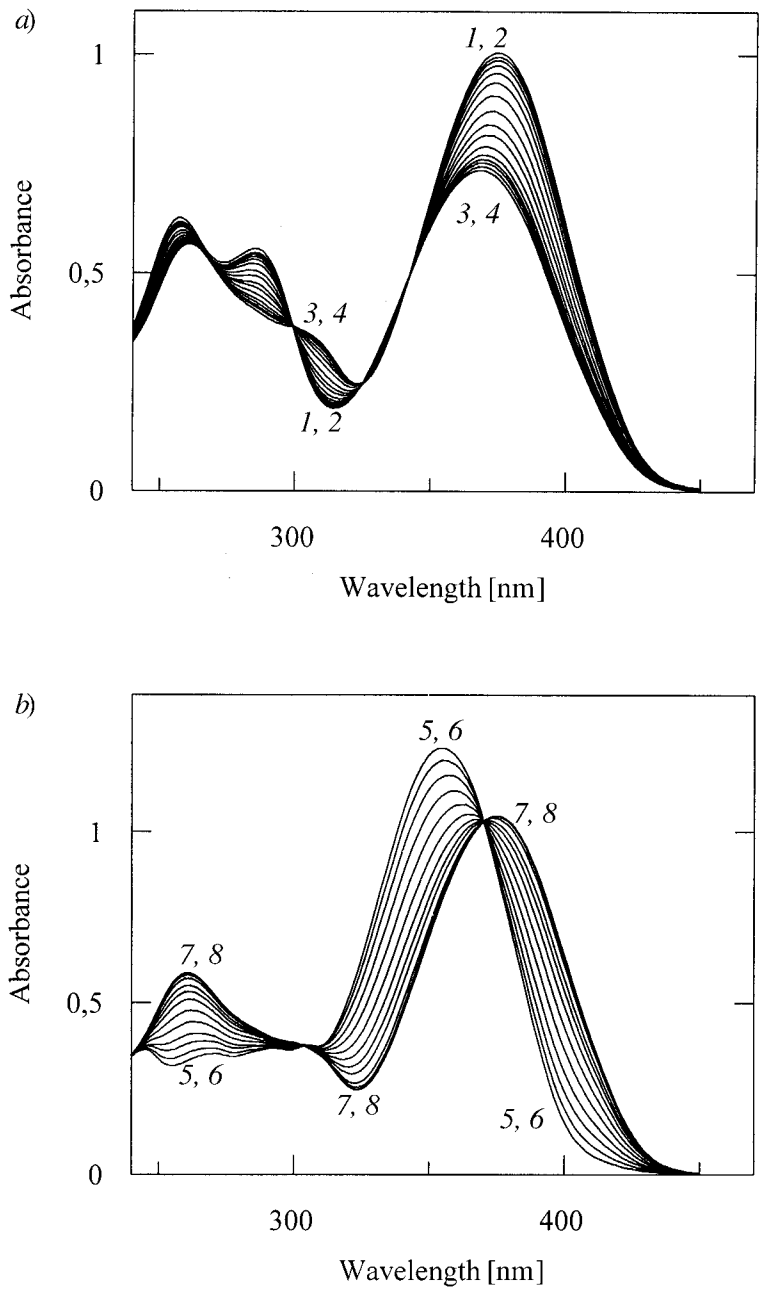

Fig. 1. *a*) *Absorption spectra of tenoxicam at 25° in the high-pH region, where the species Hten⁻* (λ_{max} 370 nm) *and H_2ten* (λ_{max} 375.5 nm) *are present: pH 3.19 and 3.79 for curves* **1** *and* **2**, *respectively, and pH 6.64 and 10.00 for curves* **3** *and* **4**, *respectively. b*) *Absorption spectra of tenoxicam at 25° in the low-pH region, where the species H_2ten* (λ_{max} 375.5 nm) *and H_3ten⁺* (λ_{max} 362.5 nm) *are present: pH 0.39 and 0.59 for curves* **5** *and* **6**, *respectively, and pH 3.39 and 3.70 for curves* **7** *and* **8**, *respectively.*

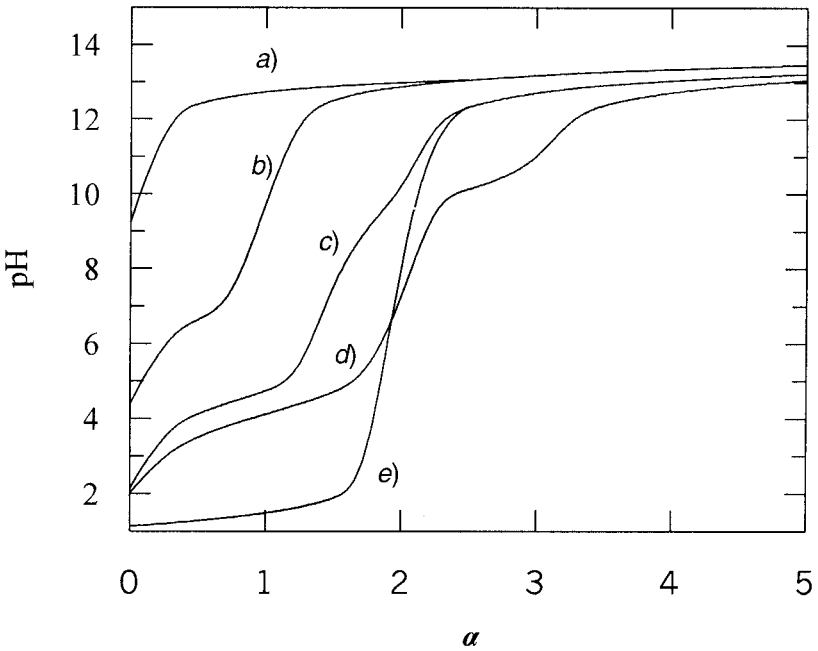

Fig. 2. *Potentiometric titration curves at 25° in $CHCl_3$/MeOH 1:1 (v/v) with KOH:* a) *free solvent,* b) *tenoxicam* (10^{-3} M), c) *$SnBu_2Cl_2$* (10^{-3} M), *d) tenoxicam* (10^{-3} M) *and $SnBu_2Cl_2$* (10^{-3} M), *and $SnBu_2Cl_2$* (10^{-3} M), *and* e) *HCl* ($2 \cdot 10^{-3}$ M). α = Mol of base added per mol of ligand or gram-ion of metal.

strongly defined equivalence point for a HCl solution of double the amount of tenoxicam or $SnBu_2Cl_2$ (*Fig. 2,e*). Still, curve *d* lies between the curves *c* and *e* (see *Fig. 2*). All these mean that tenoxicam and $SnBu_2Cl_2$ initially do not react quantitatively, but during the titration, two tenoxicam protons are finally released and neutralized. It is stressed that tenoxicam cannot be doubly ionized in the absence of diorganotin(IV). Beyond the first end point, a slow downward drift of the pH measurements is noted upon the addition of KOH, and a second inflection point appears. This is probably the result of an alkaline hydrolysis of the chelate according to *Eqn. 7.*

$$[SnBu_2(ten)] + KOH \rightarrow SnBu_2O + KHten \quad (7)$$

First, a white solid was precipitated and separated. The solid was identified by its IR data as $SnBu_2O$. Then, the solution was partially evaporated, and a slightly yellow solid was precipitated, isolated, and identified as KHten by IR data and, in aqueous solutions, by spectrophotometry. It is important to note that the amount of KOH used is critical: it cannot be more than twice the amount of tenoxicam because the chelate is dissociated, but it cannot be less either because the chelation of tenoxicam and $SnBu_2Cl_2$ would be incomplete.

Structural Characterization. The organotin adducts **1** and **2** were prepared in benzene solution according to the reactions shown in *Eqns. 8* and *9*.

$$SnBu_2O + H_2ten \rightarrow [SnBu_2(ten)] + H_2O \quad (8)$$

$$SnBu_2O + 2\ H_2ten \rightarrow [SnBu_2(Hten)_2] + H_2O \quad (9)$$

The stoichiometries of the complexes indicate that organotin(IV) is coordinated by the singly charged anion $Hten^-$ in $[SnBu_2(Hten)_2]$ (**2**) and by the doubly charged anion ten^{2-} in $[SnBu_2(ten)]$ (**1**).

The molecular structure of **1** with the atom-numbering scheme is shown in *Fig. 3*. $[SnBu_2(ten)]_n$ has 1:1 Sn/ten stoichiometry, and the doubly deprotonated ligand ten^{2-} is coordinated as a tridentate ligand *via* the enolic O-atom O(4) and the amide N(31) and pyridinyl N(1′) N-atoms. Two butyl C-atoms complete the five-coordination of the diorganotin(IV) fragment. The intramolecular Sn–O bond length, 2.094(3) Å (see *Table 2*), corresponds well to the single covalent radius value of *ca.* 2.0 Å and reflects strong coordination bonds [8][14a]. The Sn–N(Py) bond distance is 2.426(4) Å,

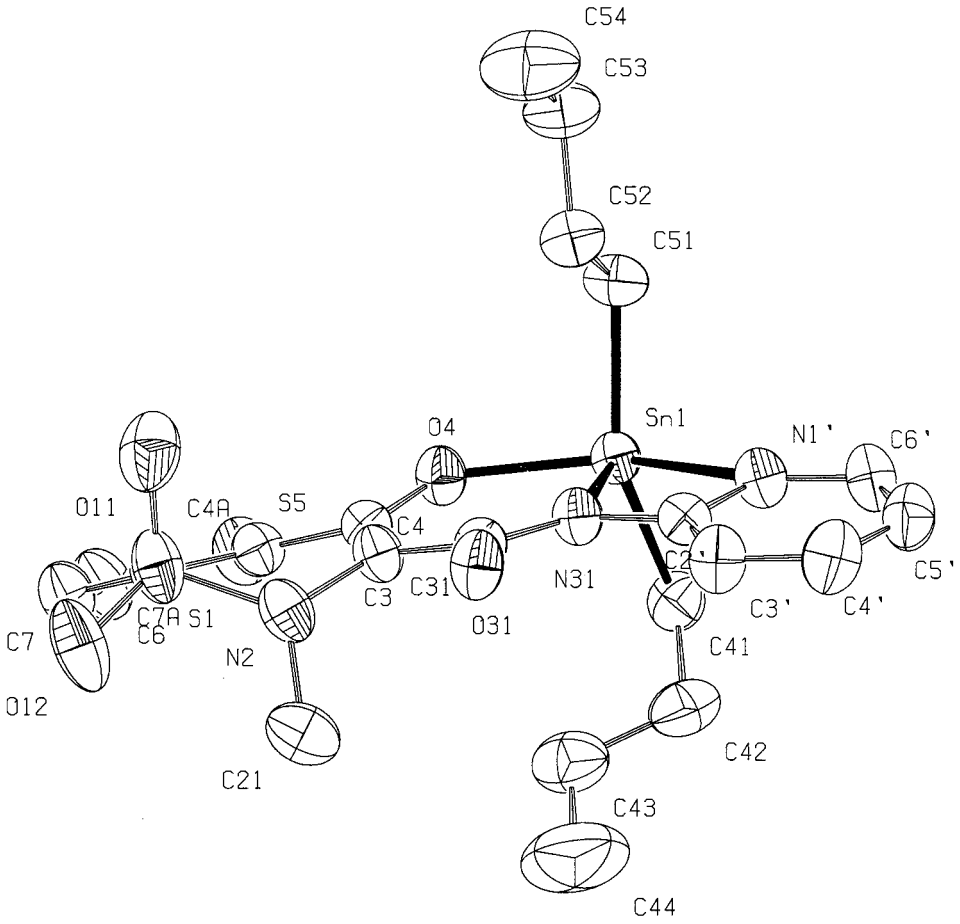

Fig. 3. *ORTEP Representation of* **1** *with the atom-numbering scheme*

Table 2. *Selected Bond Lengths* [Å] *and Angles* [deg] *for [$SnBu_2$(ten)]* (**1**)

Bond lengths			
Sn(1)–O(4)	2.094(3)	N(2)–C(3)	1.447(5)
Sn(1)–C(51)	2.112(4)	N(2)–C(21)	1.472(7)
Sn(1)–C(41)	2.122(4)	C(31)–O(31)	1.232(5)
Sn(1)–N(31)	2.159(3)	C(4)–O(4)	1.309(5)
Sn(1)–N(1′)	2.426(3)	O(1S)–C(1S)	1.25(3)
Angles			
O(4)–Sn(1)–C(51)	96.5(2)	C(6′)–N(1′)–Sn(1)	148.7(3)
O(4)–Sn(1)–C(41)	100.4(2)	C(21)–N(1′)–Sn(1)	91.6(2)
C(51)–Sn(1)–C(41)	147.5(2)	C(4)–O(4)–Sn(1)	128.5(2)
O(4)–Sn(1)–N(31)	83.63(11)	C(42)–C(41)–Sn(1)	115.1(3)
C(51)–Sn(1)–N(31)	103.77(14)	C(52)–C(51)–Sn(1)	113.7(3)
C(41)–Sn(1)–N(31)	105.5(2)	C(31)–N(31)–Sn(1)	134.3(3)
O(4)–Sn(1)–N(1′)	141.31(11)	C(2′)–N(31)–Sn(1)	102.5(2)
C(51)–Sn(1)–N(1′)	91.9(2)		
C(41)–Sn(1)–N(1′)	91.9(2)		
N(31)–Sn(1)–N(1′)	57.70(12)		

whereas the Sn–N(amide) distance is 2.159(3) Å. The stronger coordination by the deprotonated amide N-atom is attributed to its higher basicity. The very long Sn–N(Py) bond is readily explicable in terms of ring-strain effects in the four-membered chelate ring and as a result of the low degree of covalent character of the Sn–N(Py) bond. According to *Crow et al.*, diorganotins with Sn–N bonds longer than 2.39 Å are associated with antitumour activity. On this basis, **1** should be active [14c].

Analysis of the shape-determining angles using the approach of *Reedijk* and co-workers [15] yields a τ ($(\alpha$-$\beta)/60$) value of 0.1 ($\tau = 0.0$ and 1.0 for *sp* and *tbp* geometries, resp.). The metal-coordination geometry is, therefore, described as square pyramidal with the N(31) occupying the apical position. The donor N(31) is chosen as the apex by the simple criterion that the apex may not be any of the four donor atoms which define the two largest angles, α and β [15]. The coordinated part of the ligand is made of three rings, one heterocyclic (I) and two chelates, the 4-membered (II) and the 6-membered ring (III). The dihedral angles between the planes of the rings I and II, II and III, and I and III are 5.8(2), 2.46(18), and 8.0(2)°, respectively, indicating that the ligand as a whole deviates from planarity, the largest deviations arising from the expected puckering of the sulfonamide rings which contain the pyramidal saturated N-atoms. The C(31)–O(31) bond length indicates strongly that this bond is ketonic, which is also supported by the coplanarity of the three bonds to C(31). The dianionic, tridentate ligand has an (*E*,*Z*,*Z*)-configuration about the bonds C(2′)–N(31), N(31)–C(31), and C(31)–C(3). This type of ligand configuration was found in the complex $[SnBu_2(pir)]_n$ [11] and differs from the (*Z*,*Z*,*Z*)-isomer only by a 180° rotation of the pyridinyl ring. The deprotonation at the amide N-atom is one of the principal effects favoring the (*E*,*Z*,*Z*)-configuration.

Molecules of **1** are joined into dimers in a head-to-tail fashion by intermolecular bonds between tin and the neighbouring ketonic O-atom, with a distance Sn(1)···O(31)^i of 2.650(3) Å. The range of intermolecular distances Sn···O of 2.61–3.02 Å, having been confidently reported for intramolecular bonds, indicate Sn–O bonding

[14b]. The dimers of Sn(1) are arranged in polymers with a stacking of alternate parallel chains. Crystal cohesion is ensured by the H-bonds in and between the chains. The dimers of Sn(1) are linked through intermolecular H-bonds of the C–H···O type [16a], O(11)ax···H–C(41b), while the chains are linked through O(4)eq···H–C(7). The donor atom O(4) participates in intermolecular H-bonds linking the chains along the *a* and *b* direction. Furthermore, inter- and intramolecular C–H···π interactions [16b] and intramolecular bonds stabilize this structure. Although it is remarkable that there are so many contacts, and so many of different type, the interactions themselves are consistent with known guidelines for H-bond formation [16c]. In this case, molecular recognition of the H-bonds leads to aggregation and a supramolecular assembly. These interactions are listed in *Table 3* and are shown in the packing diagrams in *Fig. 4*. Also, *Table 3* lists other close approaches of the type C–H···π, and some intramolecular interactions.

The negative charge at the atoms in a molecule with several donor centers can be used to study its formation of a donor–acceptor bond with a metal. In H_2ten, Hten$^-$, and ten^{2-}, the four O-atoms exhibit the maximum electron density and negative charge [17]. The highest effective charge and the highest electron-density values for the four O-atoms and for the pyridinyl and deprotonated-amide N-atoms in **1** evidently show strong electron-donor properties and could rationalize the coordination scheme and the extended network of inter- and intramolecular H- and non-H-bonding. The high effective-charge and electron-density values for the enolate O-atom and the amide O-atom of Hten$^-$ also indicate strong electron-donor properties in **2**. The optimized geometry in MeCN is the one preferred over the configuration in the gas phase for H_2ten, Hten$^-$, and ten^{2-} [17]. The MeCN-solution values can be considered a good

Table 3. *Inter- and Intramolecular Hydrogen Bonding, Non-Hydrogen and C–H···π Interactions*[a])

Donor(D)	H	Acceptor (A)[b])	D···A	H···A	D–H···A
C(7)	H(7)	O(4)^{iii}	3.354(5)	2.594(5)	139.3(5)
C(41)	H(41B)	O(11)^{i}	3.381(6)	2.479(6)	154.5(4)
C(3′)	H(3′)	O(31)	2.835(6)	2.302(6)	116.0(5)
C(21)	H(21A)	O(12)	2.838(8)	2.404(8)	107.0(5)
Sn(1)		O(31)^{i}	2.650(3)		
Sn(1)		C(31)^{i}	3.632(4)		
O(31)		C(41)^{ii}	3.006(5)		
O(31)		C(51)^{ii}	3.004(5)		
			H···Cg	X···Cg	C–H···Cg
C(5′)–H(5′)→Cg(1)^{iv}[b])			3.329	4.093	140.92
C(53)–H(53B)→Cg(4)^{v}[b])			2.997	3.808	141.98
C(42)–H(42B)→Cg(2)			2.637	3.138	112.46
C(43)–H(43A)→Cg(3)			2.446	3.335	152.10
C(52)–H(52A)→Cg(2)			3.228	3.183	78.67
C(52)–H(52A)→Cg(3)			2.922	3.464	116.36
C(52)–H(52B)→Cg(2)			2.838	3.183	101.96

[a]) Cg(1) and Cg(2) are the centroids of the six- and four-membered rings N(1′)–C(2′)–C(3′)–C(4′)–C(5′)–C(6′) and Sn(1)–N(31)–C(2′)–N(1′), respectively; Cg(3) and Cg(4) are the six- and five-membered rings Sn(1)–N(31)–C(31)–C(3)–C(4)–O(4) and S(5)–C(4A)–C(7A)–C(7)–C(6), respectively. [b]) Symmetry operations: *i*, 1/2 – *x*,1/2 – *y*, – 1/2 + *z*; *ii*, 1/2 – *x*,1/2 – *y*,1/2 + *z*; *iii*, *y*,1 – *x*, – *z*; *iv*, *y*, – *x*, – *z*; *v*, 1 – *y*,*x*, – *z*.

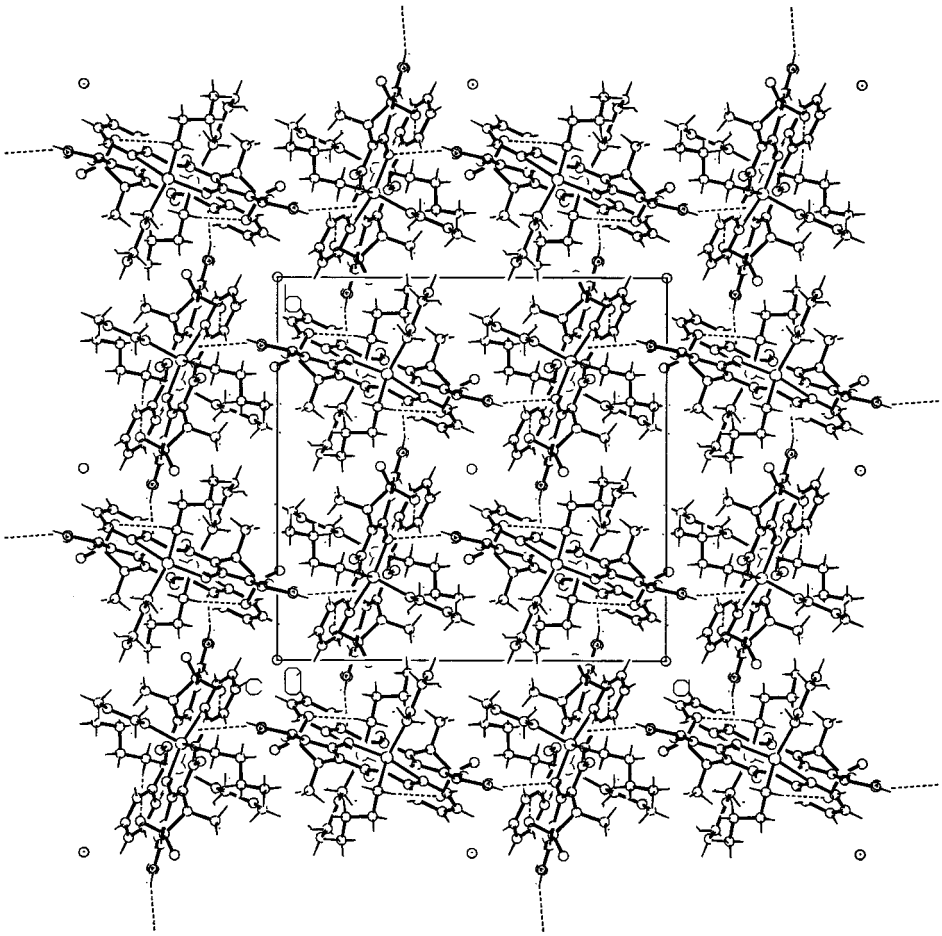

Fig. 4. *Packing diagram of the complex [SnBu$_2$ten]* (**1**) *viewed along the* a *axis of the unit cell, showing intra- and inter-molecular H-bonds*

approximation of the relative stability of the species in MeCN/MeOH. For ten^{2-}, a dramatic difference in stability results in MeCN and, in general, polar solvents. The relative stability was computed as -61.9 and -270 kcal · mol^{-1} for the dianionic species in the gas phase and in MeCN solution, respectively. The total dipole moment and the enthalpy of formation of the neutral (H_2ten) and doubly deprotonated tenoxicam (ten^{2-}) in the gas phase, as have been calculated from MOPAC93 [17], are given in *Fig. 5*.

Spectroscopy. – *Infrared Spectroscopy.* The ligand H_2ten shows a broad absorption band centred at *ca.* 3450 cm^{-1} characteristic of an O–H stretching vibration. The band at 3065 cm^{-1} for tenoxicam is attributed to the N–H stretching vibration. The low frequency of these two bands may be explained by inter- and intramolecular H-bonds

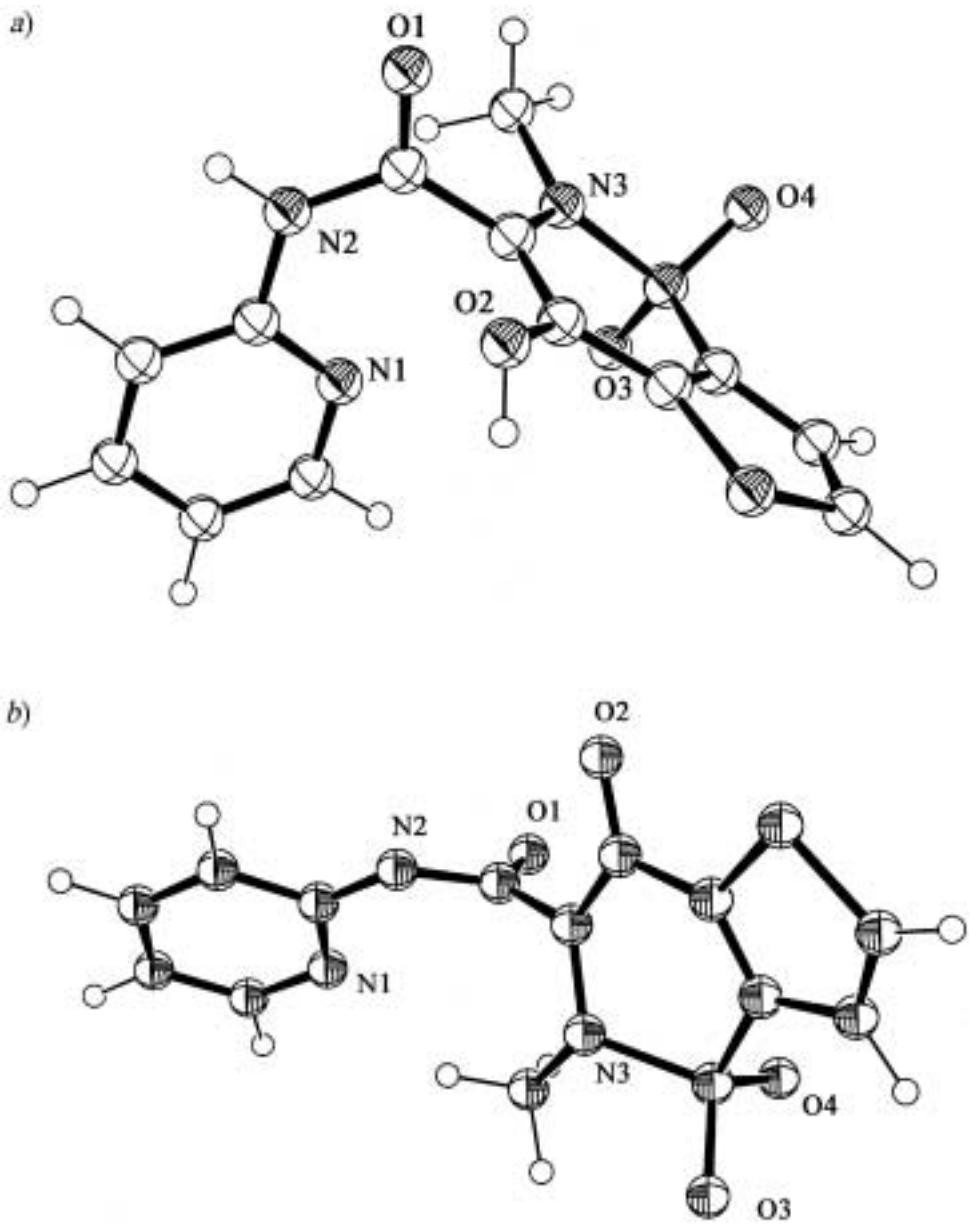

Fig. 5. *Fully PM3-optimized geometry of* a) *the neutral* (H_2ten) *and* b) *the doubly deprotonated* (ten^{2-}) *tenoxicam* ($\Delta H_f = -54.06$ kcal mol^{-1}, and dipole moment = 5.36 Debye and $\Delta H_f = -61.89$ kcal mol^{-1} and dipole moment = 9.28 Debye, resp.) *in the gas phase*

involving the N- and two O-atoms of the secondary amide group [18a]. These results agree with the crystal structure of the neutral molecule, where the neutral molecule exists in the zwitterionic form, adopting a planar conformation that is stabilized by two

intramolecular H-bonds (N–H···O) [6]. The sharp bands observed at 1653 and 1639 cm^{-1} and the band at 1596 cm^{-1} in tenoxicam are assigned to the C=O and C=N stretching vibrations of the secondary amide group –CO–NH– [18]. The $\tilde{\nu}$(C=O) and the $\tilde{\nu}$(C=N) bands are at lower frequencies in the complexes at 1600 and 1560 cm^{-1} for **1** and at 1638, 1599, and 1560 cm^{-1} for **2**. For compounds **1** and **2**, bands assignable to $\tilde{\nu}_{asym}$ and $\tilde{\nu}_{sym}$(Sn–C_2) are observed at 507, 478 and 516, 479 cm^{-1}, respectively, indicating a nonlinear Sn–C_2 moiety. The bands at 237 and 217 cm^{-1} for **1** are assigned to the $\tilde{\nu}$(Sn–N(Py)) and $\tilde{\nu}$(Sn–O) stretching modes, and the bands at 216 and 206 cm^{-1} for **2** are assigned to the $\tilde{\nu}$(Sn–O) stretching modes [9].

NMR Spectroscopy. ^{1}H- and ^{13}C-NMR spectra were recorded for tenoxicam, **1**, and **2** in $CDCl_3$. The ^{1}H-NMR parameters for donor [18a] and adducts are given in *Table 4*. Peak assignments were based on 2D-NMR data (^{1}H,^{1}H-COSY and ^{1}H,^{13}C-HETCOR; see *Fig. 6*). In complex **1**, the deshielding to *ortho* proton H–C(6′) (8.51 ppm) and C(6′) (141.9 ppm) is observed, which should be related to the electrophilicity of the tin. A σ-charge donation from the N(1′) donor to the Sn center removes electron density from the ligand and produces this deshielding, which attenuates at positions remote from the metal. The upfield shift observed for H–C(4′) and C(4′), *para* to the Sn center, could be due to the flow of charge from the Sn into the aromatic ring (π-back donation) [19b]. The signals corresponding to the NH and OH groups disappear upon interaction with the metal, indicating deprotonation at these positions and possible coordination to the Sn-atom. A tridentate coordination *via* the enolic O-atom and the amide and the pyridinyl N-atoms has recently been observed for the first time in a similar complex of piroxicam, $[SnBu_2(Pir)]_n$, where the ligand exists also in its doubly deprotonated form. These conclusions are confirmed by the ^{13}C-NMR spectrum where the C(4) signal disappears, while the C(3) signal shows a significant downfield shift of 5.2 ppm in the complex. A similar shift is observed for C(6) (6.2 ppm). The bond development between N(1′) and the Sn-atom leads to a downfield shift by 3.4 ppm of C(6′), while C(4′) shifts in the opposite direction by 5.0 ppm. From the ^1J(C,Sn) coupling constant observed for this complex, an angle of 129° can be calculated from the relationship $|\,^1J(^{119}Sn,^{13}C)| = (9.99 \pm 0.73)\theta - (746 \pm 100)$ established for tetra-, penta-, and hexa-coordinated butyltin(IV) compounds [19c].

Both ^{1}H- and ^{13}C-NMR spectra clearly show the existence of three signals for most of the ligand atoms. One is attributed to the free drug, H_2ten, implying that the complex is partially dissociated in $CDCl_3$ solution. The simultaneous presence of two structural isomers [19c] or two different complexes could be concluded. If we call them *Complex a* and *Complex b*, peak integration gives the following ratio: *Complex b*/free ligand/*Complex a* 1:1:3. Looking at the resonances corresponding to *Complex a*, we observe that they match exactly those found for the complex $[SnBu_2(ten)]$ (**1**) described above, so we draw the conclusion that, in $CDCl_3$ solution, $[SnBu_2(Hten)_2]$ (**2**) loses one ligand, and after bond rearrangement, it gives $[SnBu_2(ten)]$ (**1**), according to *Eqn. 10*.

$$[SnBu_2(Hten)_2] \rightleftharpoons H_2ten + [SnBu_2(ten)] \tag{10}$$

J(Sn,C) Coupling constants for $[SnBu_2(ten)]$ (**1**) and *Complex a* are also the same. *Complex b*, which should be $[SnBu_2(Hten)_2]$ (**2**), shows deprotonation at only the OH

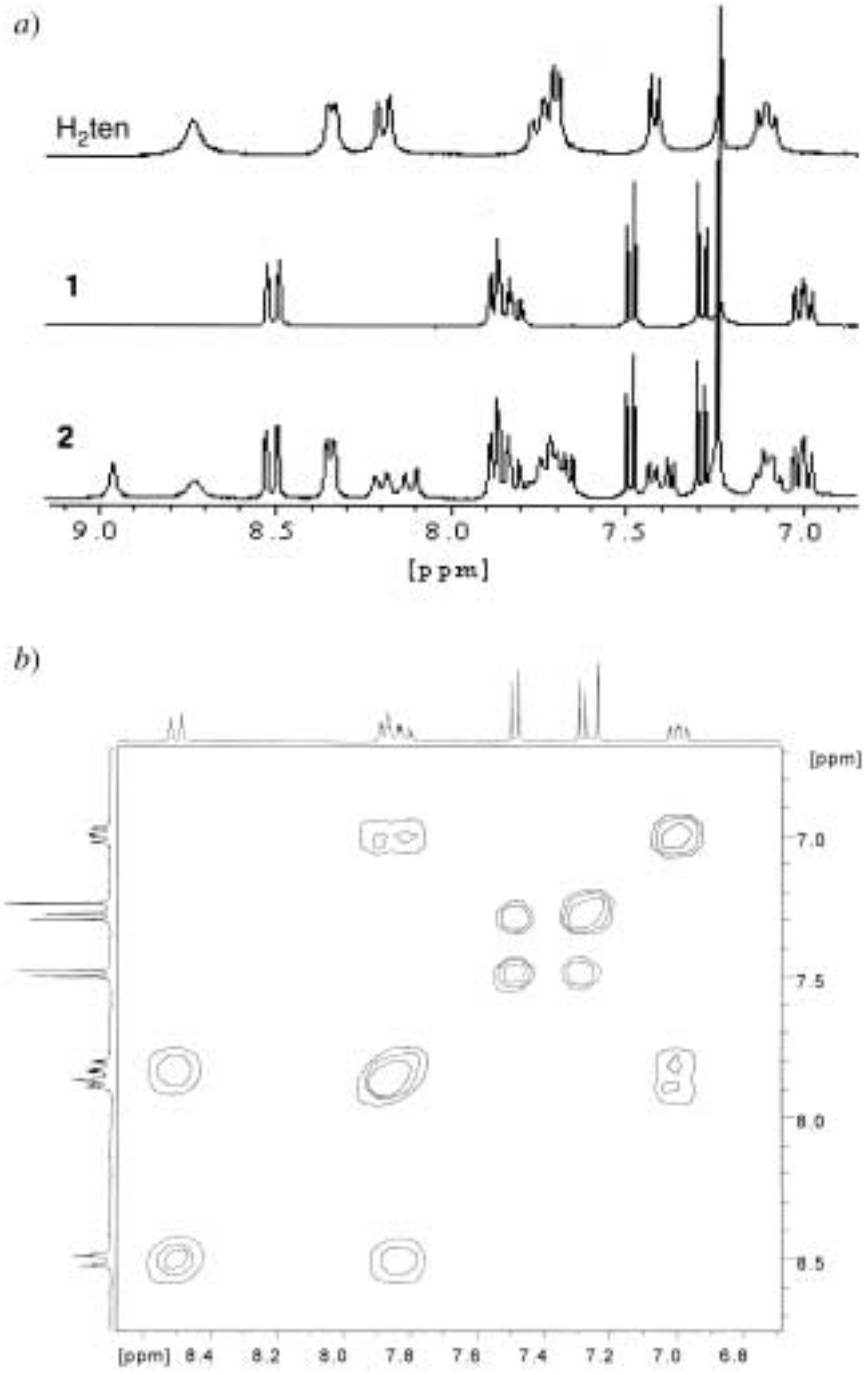

Fig. 6. a) *^{1}H-NMR Spectra of H_2ten*, **1**, *and* **2** *and* b) *2D ^{1}H,^{1}H-COSY NMR Data of* **1**

Table 4. *^{1}H-NMR Parameters of Tenoxicam and the Complexes* **1** *and* **2** (δ in ppm and J in Hz)

	H–C(3′)	H–C(4′)	H–C(5′)	H–C(6′)	H–C(7)	H–C(8)	Other
H_2ten[a])	7.73 ($d, J = 8.4$)	8.17 ($t, J = 7.7$)	7.33 ($t, J = 6.5$)	8.34 ($d, J = 5.6$)	7.46 ($d, J = 4.9$)	8.03 ($d, J = 5.0$)	13.79 (br., OH)
H_2ten[b])	7.70 ($d, J = 4.9$)	8.20 ($d, J = 8.2$)	7.11 ($t, J = 7.1$)	8.35 ($d, J = 3.8$)	7.42 ($d, J = 4.9$)	7.76 ($t, J = 7.1$)	13.79 (br., OH) 8.74 (br., NH)
1[b])	7.88 ($d, J = 7.1$)	7.83 (t)	7.00 ($t, J = 7.1$)	8.51 ($d, J = 8.2$)	7.29	7.49 ($d, J = 5.5$)	0.87 (Me) 1.32 (MeCH_2CH$_2$CH$_2$) 1.62 (MeCH$_2$CH_2CH$_2$)
2[b])[c])	8.12 (d)	7.84 (t)	7.00 (t)	8.34 (d)	7.38 (d)	7.66 (d)	8.93 (NH) 0.74 (t, Me) 1.38 (MeCH_2CH$_2$CH$_2$) 1.62 (MeCH$_2$CH_2CH$_2$)

[a]) In (D_6)DMSO. [b]) In $CDCl_3$. [c]) The peaks corresponding to **2** are referred.

group as the amide NH peak appears at 8.93 ppm. Coordination of the metal to O(4) is concluded.

D.K.-D. thanks '*HELP EPE*' for the generous gift of tenoxicam. We thank *GSRD* for a grant *PENED* No 820.

REFERENCES

[1] J. F. Gonzales, P. A. Todd, *Drugs* **1987**, *34*, 298; 'The Merck Index', 11th edn., Merck, Rahway, NJ, USA, 1989, p. 1441.
[2] T. F. Woolf, L. L. Radulovic, *Drug Metab. Rev.* **1989**, *21*, 255.
[3] P. Heizmann, J. Korner, K. Kinapold, *J. Chromatogr. Biomed. Appl.* **1986**, *374*, 95.
[4] R.-S. Tsai, P.-A. Carrupt, N. El Tayar, Y. Giroud, P. Adrade, B. Testa, F. Brée, J.-P. Tillement, *Helv. Chim. Acta* **1993**, *76*, 842.
[5] A. Bury, A. E. Underhill, D. R. Kemp, N. J. O'Shea, J. P. Smith, P. S. Gomm, *Inorg. Chim. Acta* **1987**, *138*, 85.
[6] M. R. Caira, L. R. Nassimbeni, M. Timme, *J. Pharm. Sci*. **1995**, *84*, 884.
[7] E. Bernhard, F. Zimmermann, *Arzneim.-Forsch. Drug Res.* **1984**, *34*, 647.
[8] J. J. Zuckerman (Ed.), 'Organotin Compounds: New Chemistry and Applications', Advances in Chemistry Series, no 157, American Chemical Society, Washington, 1976; C. J. Evans, S. Karpel, 'Organotin Compounds in Modern Technology', J. Organomet. Chem. Library 16, Elsevier, 1985; S. J. Blunden, P. A. Cusack, R. Hill, 'Industrial Uses of Tin Chemicals', Royal Society of Chemistry, London, 1985; A. J. Crowe, in 'Metal-Based Antitumour Drugs', Ed. M. Gielen, Freund, London, 1989, Vol. 1, p. 103.
[9] P. Tauridou, U. Russo, G. Valle, D. Kovala-Demertzi, *J. Organomet. Chem*. **1993**, *44*, C16; D. Kovala-Demertzi, P. Tauridou, J. M. Tsangaris, A. Moukarika, *Main Group Met. Chem.* **1993**, *5*, 315; P. Tauridou, U. Russo, D. Marton, G. Valle, D. Kovala-Demertzi, *Inorg. Chim. Acta* **1995**, *231*, 139; D. Kovala-Demertzi, P. Tauridou, A. Moukarika, J. M. Tsangaris, C. P. Raptopoulou, A. Terzis, *J. Chem. Soc.*, *Dalton Trans*. **1995**, 123; D. Kovala-Demertzi, P. Tauridou, U. Russo, M. Gielen, *Inorg. Chim. Acta* **1995**, *239*, 177; N. Kourkoumelis, A. Hatzidimitriou, D. Kovala-Demertzi, *J. Organomet. Chem*. **1996**, *514*, 163; D. Kovala-Demertzi, N. Kourkoumelis, P. Tavridou, A. Moukarika, P. D. Akrivos, U. Russo, *Spectrochim. Acta.*, *Part A* **1998**, *54*, 180.
[10] a) D. Kovala-Demertzi, A. Theodorou, M. A. Demertzis, C. Raptopoulou, A. Terzis, *J. Inorg. Biochem.* **1997**, *6*, 151; b) D. Kovala-Demertzi, D. Mentzafos, A. Terzis, *Polyhedron* **1993**, *11*, 1361; c) D. Kovala-Demertzi, S. K. Hadjikakou, M. A. Demertzis, Y. Deligiannakis, *J. Inorg. Biochem.* **1998**, *69*, 223; d) M. Konstandinidou, A. Kourounakis, M. Yiangou, L. Hadjipetrou, D. Kovala-Demertzi, S. K. Hadjikakou,

M. A. Demertzis, *J. Inorg. Biochem.* **1998**, *70*, 63; e) A. Theodorou, M. A. Demertzis, D. Kovala-Demertzi, E. E. Lioliou, A. Pantazaki, D. A. Kyriakidis, *Biometals* **1999**, *12*, 167.

[11] S. K. Hadjikakou, M. A. Demertzis, J. R. Miller, D. Kovala-Demertzi, *J. Chem. Soc., Dalton Trans.* **1999**, 663.

[12] a) 'KUMA KM-4 Software, Version 5.0', Kuma Diffraction, Wroclaw, Poland 1992; b) G. M. Sheldrick, *Acta Crystallogr. Sect. A* **1990**, *46*, 467; c) G. M. Sheldick, 'SHELXL93, Program for the Refinement of Crystal Structures,' University of Göttingen, Germany, 1993; A. L. Spek, 'PLATON, A Program for the Automated Generation of a Variety of Geometrical Entities', University of Utrecht, The Netherlands, 1997.

[13] a) D. Kovala-Demertzi, M. A. Demertzis, P. Nath Yadav, A. Castineiras, D. X. West, *Transition Met. Chem. (London)* **1999**, *24*, 642; b) G. D. Christian, 'Analytical Chemistry', 4th edn., John Wiley & Sons, Inc., New York, 1986, p. 303; c) R. W. Ramette, 'Chemical Equilibrium and Analysis', Addison-Wesley Publishing Company, London, 1981, p. 432.

[14] a) K. C. Mollow, T. G. Purcell, K. Quill, I. W. Nowell, *J. Organomet. Chem.* **1984**, *267*, 237; b) A. R. Forrester, S. J. Garden, R. A. Howie, J. L. Wardell, *J. Chem. Soc., Dalton Trans.* **1992**, 2615; c) A. J. Crow, P. J. Smith, C. J. Cardin, H. E. Parge, F. E. Smith, *Cancer Lett*. **1984**, *24*, 45.

[15] A. Addison, R. T. Nageswara, J. Reedijk, J. Van Rijn and G. C. Verschoor, *J. Chem. Soc., Dalton Trans.* **1984**, 1349.

[16] a) T. Steiner, B. Lutz, J. van der Maas, A. M. M. Schreurs, J. Kroon, M. Tamm, *Chem. Commun*. **1998**, 171; b) T. Steiner, M. Tamm, A. Grzegorzewski, N. Schulte, N. Veldman, A. M. M. Schreurs, J. Kroon, J. van der Maas, B. Lutz, *J. Chem. Soc., Perkin Trans.* **1996**, 2441; c) M. C. Etter, *Acc. Chem. Res* **1990**, *23*, 120; d) G. R. Desiraju, *Acc. Chem. Res.* **1991**, *24*, 290.

[17] J. J. P. Stewart, *J. Comput. Chem.* **1989**, *10*, 210; J. Baker, *J. Comput. Chem.* **1985**, *7*, 385; J. J. P. Stewart, 'MOPAC93', Fujitsu, 1993.

[18] a) L. J. Bellamy, 'The Infrared Spectra of Complex Molecules', Chapman and Hall, London, 1975; b) K. Nakamoto, 'Infrared and Raman Spectra of Inorganic and Coordination Compounds', 4th edn., Wiley, New York, 1980; c) G. Maistralis, N. Katsaros, S. P. Perlepes, D. Kovala-Demertzi, *J. Inorg. Biochem.* **1992**, *45*, 1.

[19] a) H. Tai-jun, Z. Zheng-xing, *Zhongguo Yaoke Daxue Xuebao* **1997**, *28*, 285; b) A. G. Quiroga, J. M. Perez, I. Lopez-Solera, J. R. Masaguer, A. Luque, P. Roman, A. Edwards, C. Alonso, C. Navarro-Ranninger, *J. Med. Chem.* **1998**, *41*, 9, 1399; c) A. Pellerito, T. Fiore, C. Pellerito, A. Fontana, R. Di Stefano, L. Pellerito, M. T. Cambria, C. Mansueto, *J. Inorg. Biochem*. **1998**, *72*, 115; J. Holecek, A. Lycka, *Inorg. Chim. Acta* **1986**, *118*, L15.

Received March 31, 2000